

DNA Binding Studies of Ni(II) Complex of (E-2-Chloro-N-(3-Hydroxy-5-Hydroxymethyl)-2-Methylpyridin-4-Yl)Methylene) Acetohydrazide

Mohammed Fadhil Eesee

M.Sc, Inorganic Chemistry, Department Of Chemistry

Nizam College, Osmania University, India

ABSTRACT:

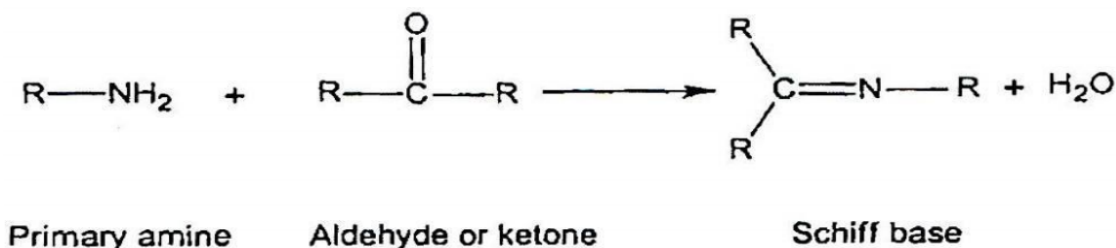
(E-2-chloro-N-(3-hydroxy-5-hydroxymethyl)-2-methylpyridin-4yl)methylene) acetohydrazide, a derivative of pyridoxal was synthesized by conventional method by treating Pyridoxal hydrochloride with Chloroacetic hydrazide. Ni(II) metal complex was synthesized and characterized using LC-MS, UV, IR and TGA methods. IR spectrum of the complex revealed that the ligand coordinated through 'N' and 'O' donor atoms.

The complex was tested for DNA binding activity using Electronic Absorption spectroscopy and Viscosity measurements. The interaction of metal complexes with CT-DNA was studied and the binding constant (K_b) was calculated.

Keywords: Acetohydrazide, Chloroacetic hydrazide. Ni(II), DNA, Donor atoms

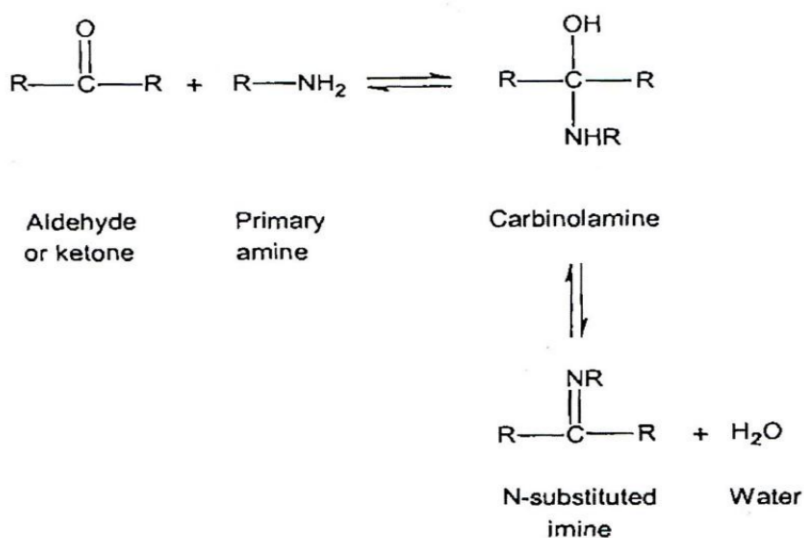
INTRODUCTION

A Schiff base is a nitrogen analog of an aldehyde or ketone in which the C=O group is replaced by C=N-R group. It is usually formed by condensation of an aldehyde or ketone with a primary amine

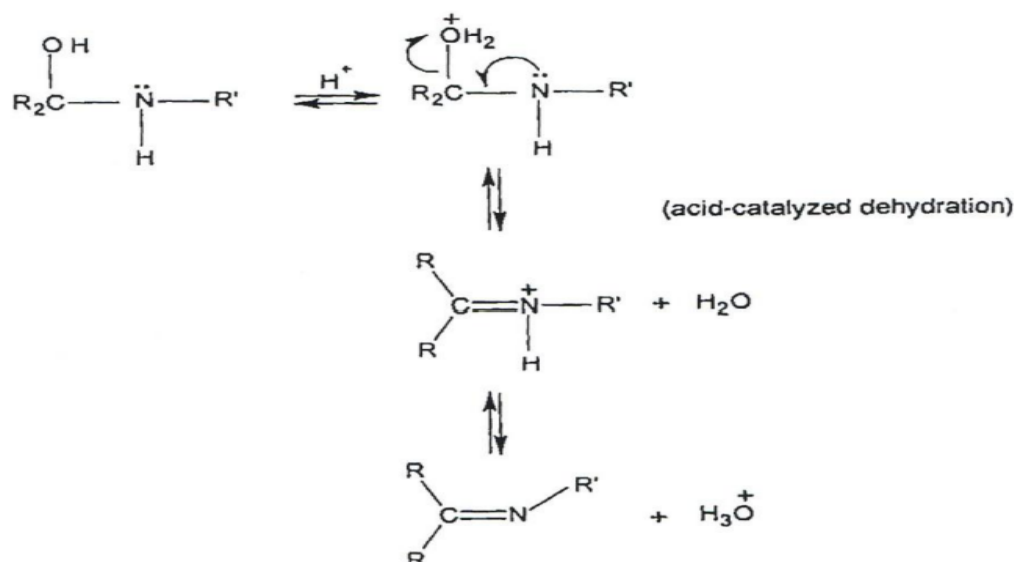


Where R, may be an alkyl or an aryl group. Schiff bases that contain aryl substituents are substantially more stable and more readily synthesized, while those which contain alkyl substituents are relatively unstable. Schiff bases of aliphatic aldehydes are relatively unstable and readily polymerizable^{1,2} while those of aromatic aldehydes having effective conjugation.

The formation of a Schiff base from an aldehydes or ketones is a reversible reaction and generally takes place under acid or base catalysis, or upon heating.



The formation is generally driven to the completion by separation of the product or removal of water, or both. Many Schiff bases can be hydrolyzed back to their aldehydes or ketones and amines by aqueous acid or base. The mechanism of Schiff base formation is another variation on the theme of nucleophilic addition to the carbonyl group. In this case, the nucleophile is the amine. In the first part of the mechanism, the amine reacts with the aldehyde or ketone to give an unstable addition compound called carbinolamine. The carbinolamine loses water by either acid or base catalyzed pathways. Since the carbinolamine is an alcohol, it undergoes acid catalyzed dehydration.



Typically the dehydration of the carbinolamine is the rate-determining step of Schiff base formation and that is why the reaction is catalyzed by acids. Yet the acid concentration cannot be too high because amines are basic compounds. If the amine is protonated and becomes non-nucleophilic, equilibrium is pulled to the left and carbinolamine formation cannot occur. Therefore, many Schiff bases synthesis are best carried out at mildly acidic pH. The dehydration of carbinolamines is also catalyzed by base. This reaction is somewhat analogous to the E2 elimination of alkyl halides except that it is not a concerted reaction. It proceeds in two steps through an anionic intermediate. The Schiff base formation is really a sequence of two types of reactions, i.e. addition followed by elimination⁷

Synthesis of Schiff bases

The first preparation of imines was reported in the 19th century by Schiff (1864). Since then a variety of methods for the synthesis of imines have been described. The classical synthesis reported by Schiff involves the condensation of a carbonyl compound with an amine under

azeotropic distillation. Molecular sieves are then used to completely remove water formed in the system. In the 1990s and *in situ* method for water elimination was developed, using dehydrating solvents such as tetramethyl orthosilicate or trimethyl orthoformate. In 2004, Chakraborti et al. demonstrated that the efficiency of these methods is dependent

on the use of highly electrophilic carbonyl compounds and strongly nucleophilic amines. They proposed as an alternative the use of substances that function as Brønsted-Lowry or Lewis acids to activate the carbonyl group of aldehydes, catalyze the nucleophilic attack by amines, and dehydrate the system, eliminating water as the final step. Examples of Brønsted-Lowry or Lewis acids used for the synthesis of Schiff bases include

ZnCl₂, TiCl₄, MgSO₄-PPTS, Ti(OR)₄,
alumina, H₂SO₄, NaHCO₃,
MgSO₄, Mg(ClO₄)₂, H₃CCOOH, Er(OTf)₃, P
2O₅/Al₂O₃.

HCl In the past 12 years a number of innovations and new techniques have been reported, including solvent-free/clay/microwave irradiation, solid-state synthesis, K-10/microwave, water suspension medium, [bmim]BF₄/molecular sieves, infrared irradiation/no solvent, NaHSO₄·SiO₂/microwave/solvent-free, solvent-free/CaO/microwave, and silica/ultrasound irradiation. Among these innovations, microwave irradiation has been extensively used due to its operational simplicity, enhanced reaction rates, and great selectivity. The use of microwave irradiation commenced with the independent studies of Rousell and

Majetich groups. Microwave irradiation is less environmentally problematic than other methods because it abolishes the excessive use of aromatic solvents and the Dean-Stark apparatus for azeotropic removal of water. Another feature of this technique is that the reactions achieve high efficiency in a shorter period of time.

RELATED LITERATURE:

M. A. Neelakantan, M. Sundaram, and M. Sivasankaran Nair J. Chem. Eng. Data, 2011, 56 (5), pp 2527–2535 DOI: 10.1021/je200054w studied that Solution equilibria and relevant stability constants for M(II)-pyridoxine (PN)(A) [M(II) = Cu(II), Ni(II), and Zn(II)], and M(II)-PN(A)-imidazole containing ligands (B) [B = imidazole (him), benzimidazole (bim), histamine (hist), and l-histidine (his)] in aqueous solution have been determined by a pH metric method at 310 K and I = 0.15 M NaClO₄. The complexation model for each system has been established by the MINIQUAD-75 program. The probable binding mode in the binary and ternary species was discussed based upon the derived stability constants. The concentration distributions of various species formed in solution were evaluated. The stability of ternary

complexes follows the Irving–Williams order of metal ions, which was quantitatively ($\Delta \log K$, $\log X$, and % RS) compared with their corresponding binary complexes. In terms of the ligands (B), the stability of the complexes follows $\text{him} > \text{bim} > \text{hist} > \text{his}$. The molecular geometry of the complexes formed in solution between the ligands and M(II) was determined by electronic spectra at various pH intervals. The formation of complexes and their electrochemical properties were also assessed by cyclic voltammetry. The in vitro biological activity of the ternary complexes was tested against bacteria, fungi, and yeast.

P.R. Chetana¹ , **S. Sahana¹** , **R.S.Policegoudra²** , **Bipul Sarma³** , **Rajiv Khatioda³**; ISSN 0976 – 044X studied that This communication describes a procedure to synthesize a novel Schiff base ligand 4-chloro-2-(pyridine-3-yliminomethyl) phenol and its transition metal complexes of Cu(II) and Ni(II) and its characterization by physiochemical techniques such as elemental, FTIR, UV Visible, $^1\text{H-NMR}$, Mass spectra and cyclic voltammetry. Further, the ligand was structurally characterized by X-ray crystallography and is found to be

planar suitable for DNA studies. The complexes were screened for their in-vitro antimicrobial activity using various strains of gram positive and gram negative bacteria- *Bacillus mycoides*, *Bacillus subtilis*, *Escherichia coli*, *Micrococcus luteus*, *Proteus mirabilis*, *Pseudomonas aeruginosa* and *Yersinia enterocolitica*. The Schiff base ligand showed higher antibacterial activity than the ligand coordinated to either of the metal ion copper or nickel. The DNA cleavage studies of the complexes have been investigated and both the complexes showed extensive cleavage of DNA. However, Cu(II) complexes showed better cleavage activity compared to Ni(II) complex.

MATERIALS AND METHODS

1. PHYSICAL MEASUREMENTS

The entire chemical used were obtained from commercial source and used without purification. The IR spectra (ν , cm^{-1}) were recorded in solid state KBr dispersion using Perkin Elmer FT-IR spectrometer. The $^1\text{H-NMR}$ spectra was recorded on Bruker-Avance 500 MHz spectrometer. The chemical shifts were reported in δ/ppm relative to TMS. The mass spectra were recorded on using a Perkin Elmer

PE-SCIEX-API 2000 mass spectrometer. The reactions were monitored by Thin-layer chromatography (TLC). Melting points were determined on Polman melting point apparatus (Model No MP96) by open capillary method and are uncorrected. All the reactions were carried out under nitrogen atmosphere.

METHODS

Step-1 Preparation of chloro acetic hydrazide:

To a stirred solution at ethyl chloro acetate (3mmol) in ethanol was added hydrazine hydrate (10mmol) and refluxed for 12 hours, the reaction mixture was diluted with ethyl acetate followed by water. The organic layer was evaporated to obtain

chloro acetate hydrazide. Yield of the product is 75 %.

Step-2 Synthesis of pyridoxal chloro acetohydrazide derived from pyridoxal:

To a stirred solution of pyridoxal HCl (0.50 mmol) in ethanol was added chloro acetic hydrazide (1.0 mmol) and refluxed for 5 hours. The reaction mixture was poured into water and extracted with ethyl acetate. The organic layer was washed with water and concentrated under reduced pressure, to obtain the pure yellow coloured solid. The purity of the compounds was checked by TLC. Yields of the products 75 %.

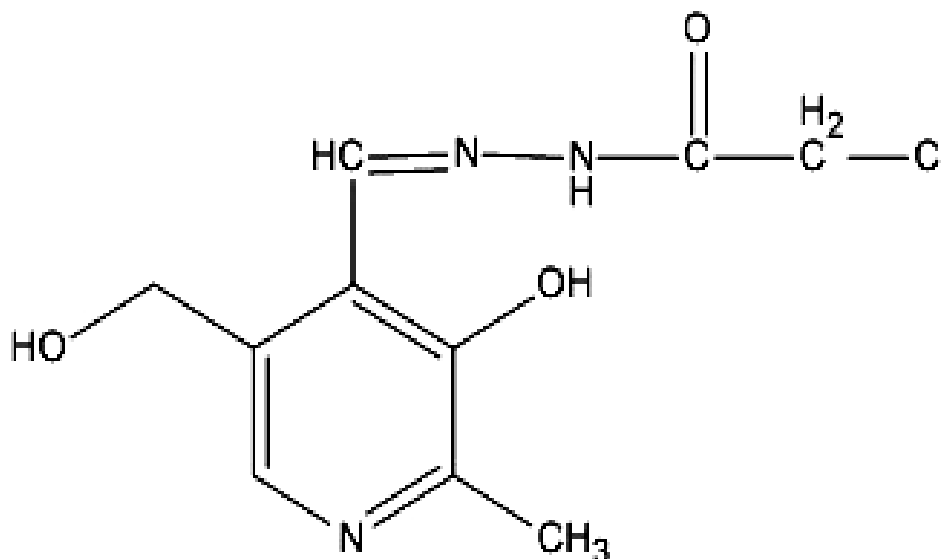


Figure 1: Structure of Pyridoxal Chloro Acetohydrazide

Synthesis of Nickel complex

Ni (II) complex of PLCAH was prepared by refluxing the metal salt solutions of Nickel chloride with hot methanolic solution of PLCAH for 15-20 hours. Molar ratio of metal to ligand ratio is 1:2. The pH was adjusted with ammonical buffer (pH=7). Solid complex separated out was washed with hot methanol, to remove unreacted ligand, then with DD water to remove unreacted metal salt and finally with petroleum ether. The solid complexes obtained was dried in a dessicator at room temperature.

Experimental techniques employed to Study Drug-DNA Interactions

UV-Visible absorption spectroscopy studies

Metal complex titration with calf thymus DNA

Electronic spectroscopy: The application of electronic absorption spectroscopy in DNA-binding studies is one of the most useful techniques. Electronic spectra indicate the nature of interaction of complexes and DNA.

The DNA concentration per nucleotide was determined by electronic absorption spectroscopy using the known molar extinction coefficient value of $6600 \text{ M}^{-1} \text{ cm}^{-1}$ at 260 nm. Absorption titration experiments of copper(II) complex samples in buffer solution (50 mM NaCl-5 mM Tris-HCl, pH 7.2) were performed by using a fixed complex concentration to which increments of the DNA stock solutions (20,40,60,80,100 μ l) were added. The Ni(II) complex-DNA solutions

were allowed to incubate for 10 minutes before the absorption study was carried out. 1mg of complex is dissolved in 1ml of DMSO and the concentration of the complex is found out using the formula,

$$M = 0.001 / \text{mol.wt}$$

of complex $\times 1000 / l = a$

The above formula gives the initial conc. of the complex solution in 1ml DMSO. The 100 μ l of this stock solution added to 3ml TRIS-HCl in a cuvette and the conc. of this solution is found out using the formula $a \times 0.1 \text{ml} = x \times 3.1 \text{ml}$ (x=conc. in 3ml)

The spectral data may suggest a groove mode of binding that involves a stacking interaction between the complex and the base pairs of DNA. In order to quantitatively compare the binding strength of the two complexes, the intrinsic binding constants K_b of the two complexes with CT DNA were determined according to the following equation

through a plot of $[DNA]/(\Sigma a - \Sigma f)$ versus $[DNA]$. $[DNA]/(\Sigma a - \Sigma f) = [DNA]/(\Sigma b - \Sigma f) + 1/K_b(\Sigma b - \Sigma f)$ where $[DNA]$ is the concentration of DNA in base pairs, the apparent absorption coefficient Σa , Σf and Σb correspond to $A_{obsd}/[Ni]$, the extinction coefficient for the nickel complex in the free and fully bound form, respectively. In plots $[DNA]/(\Sigma a - \Sigma f)$ versus $[DNA]$ K_b is given by the ratio of slope to intercept. Intrinsic binding constants K_b of Nickel complex was obtained about $4.34 \pm 0.1 \times 10^3$ from absorbance data. The binding constants indicate that binds more strongly than Zn complex.

DNA Viscosity Measurements

Viscosity Studies: Interaction between the complexes and DNA was also studied by viscosity measurements. In the absence of crystallographic structural data, hydrodynamic methods, which are sensitive to DNA length, are known to be among the some definitive & critical indicator of binding strength. Intercalation was the effect of in increasing DNA viscosity [37]. The effects of both complexes and EtBr on the viscosity of rod-like DNA are shown in Fig 6. For $[Co(en)_2bpy]^{3+}$ and $[Co(en)_2phen]^{3+}$

complexes the viscosity of DNA increases slightly with the increasing of the concentration of complex which is similar to that of proven $[Co(phen)_3]^{3+}$. Both complexes did not change the relative viscosity of DNA in a manner consistent with binding by electrostatic (or) groove mode. This result also parallels the pronounced hypochromism and spectral red shift and emission enhancement of both complexes, whereas proven classical intercalator EtBr viscosity of DNA increases with the increase of the concentration of complex. So these two complexes do not extend DNA helix length. On the basis of the viscosity results, it seems that these will bind with DNA through groove binding.

Viscosity experiments were carried out in an Ostwald viscometer maintained at $30.0 \pm 0.1^\circ C$ in a thermostatic water-bath. To minimize complexities arising from DNA flexibility. Calf thymus DNA samples ~ 200 base pairs in length were prepared by sonication. Data obtained were presented as $(\eta/\eta_0)^{1/3}$ vs the concentration of cobalt(III) complexes, where η is the viscosity of DNA in presence of complexes and η_0 is the viscosity of DNA alone. Viscosity values

were calculated from the observed flow time of DNA-containing solution ($t > 100$ s) corrected for flow time of buffer alone (t_0), $\eta = t - t_0 / t_0$. The concentrations of DNA and EtBr taken are $100 \mu\text{M}$ where as the concentration of metal complex is $25 \mu\text{M}$.

Procedure:

Electronic absorption titrations

1. Preparation of metal solution:

Stock solution of metal 1 gm in 1 ml DMSO from this 100 ml has to be diluted with 3 ml of Tris HCl buffer / phosphate buffer.

2. Keep D.D. water in refraction and Tris HCl in sample and give base line correction.

3. Tris HCl in ref. (after remaining D.D. water) DNA with buffer in sample, check reaction of absorbance at 260 nm and 280 nm = 1: 9: 1

Absorbance = calculation the concentration of DNA

4. Then Tris HCl in refraction and complex solution in sample, take absorption, then add $20 \mu\text{l}$ of DNA to both complex and Tris HCl and take absorbance after 10 min ,

Addition of DNA to both complex and Tris HCl will be: $20 \mu\text{l}$ then $40 \mu\text{l}$, $60 \mu\text{l}$, $80 \mu\text{l}$, $100 \mu\text{l}$

Viscosity Studies:

Procedure:

1. Preparation of metal solution:

Stock solution of metal 1 gm in 1 ml DMSO from this 100 ml has to be diluted with 3 ml of Tris HCl buffer / phosphate buffer.

2. Keep D.D. water in refraction and Tris HCl in sample and give base line correction.

3. Tris HCl in ref. (after remaining D.D. water) DNA with buffer in sample, check reaction of absorbance at 260 nm and 280 nm = 1: 9: 1 absorbance = calculation the concentration of DNA. 4. Fill Viscometer with buffer only (10 ml). Record time 3 times and take average. To above Viscometer add DNA $100 \mu\text{L}$. Repeat the process same as above. To this solution add Ethidium bromide in intervals of 20, 40, 60, 80, $100 \mu\text{L}$ and record the readings 3 times after each addition and take the average.

5. Fill the Viscometer with buffer 10 mL followed by DNA 100 μ L and add complex solution in the intervals of 20, 40, 60, 80, 100 μ L and record the readings 3 times after each addition and take the

average. Record time 3 times and take average.

$$\eta'_{sp} / \eta_{sp} = \{ (t_{\text{complex}} - t_0) / t_0 \} / (t_{\text{control}} - t_0) / t_0$$

RESULTS AND DISCUSSION

Characterization of PLCAH:

LC-MS: The liquid chromatogram of PLCAH showed single peak with the retention time of 0.755min. Indicating its purity (68).

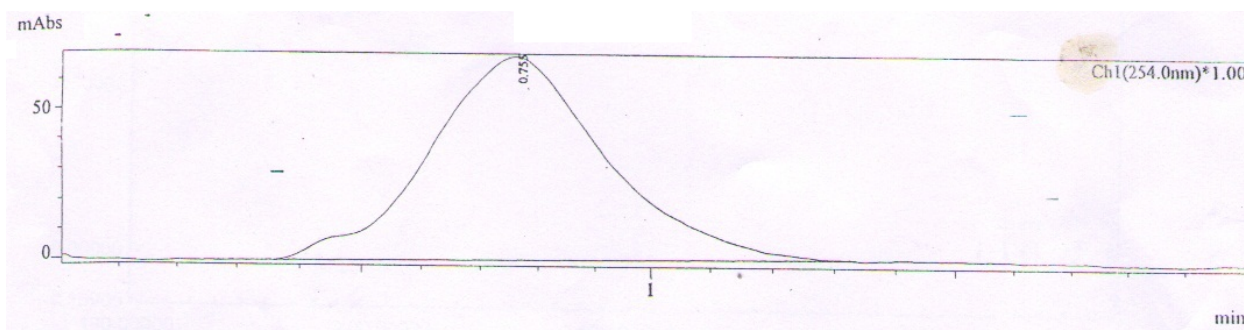


Figure 2: LC of Ligand PLCAH

ESI (+) mass spectrum showed peaks at m/z 257 indicating the molecular ion $[C_{10}H_{12}N_3O_3Cl]^+$

+

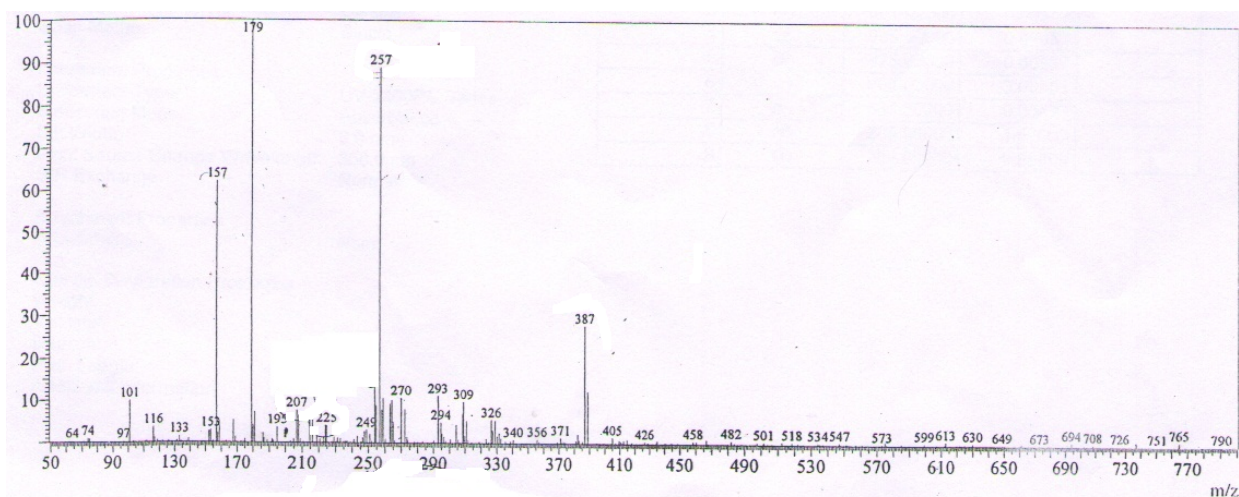


Figure 3: Mass Spectrum of Ligand PLCAH

UV spectrum:

The UV spectrum showed peak at 285nm and 252nm which correspond to $\pi \rightarrow \pi^*$ and $n \rightarrow \pi^*$ transition of the C=O group. The band at 340nm is due to C=N group.

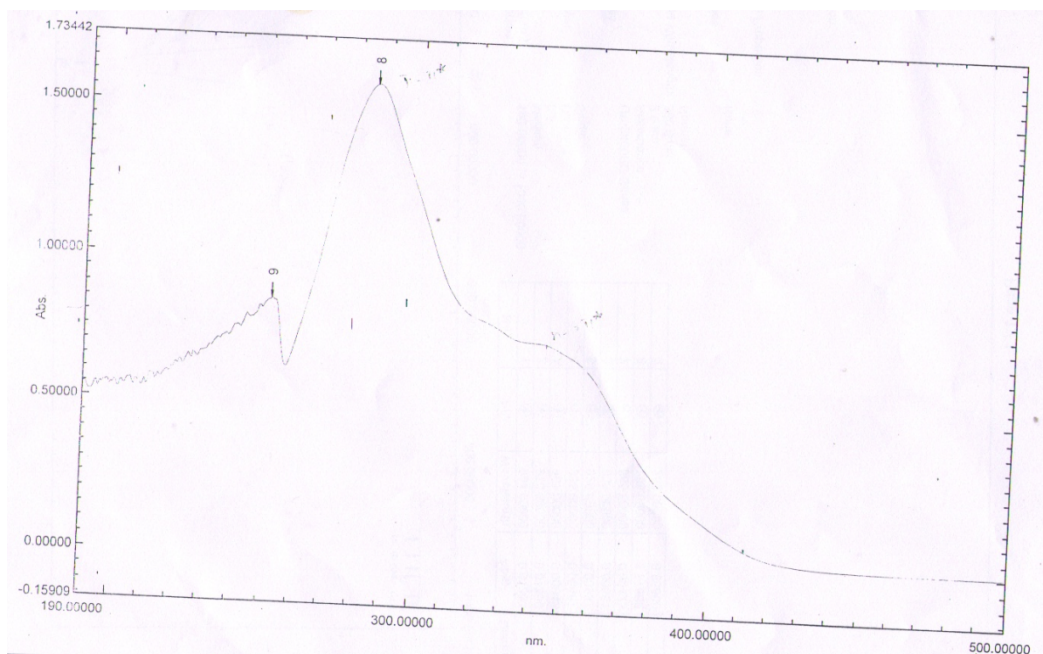


Figure 4: UV Spectrum of Ligand PLCAH

IR spectrum:

The IR spectrum of PLCAH showed the following peaks at ν 3323 cm^{-1} (OH on the pyridine ring), peak at ν 3111 cm^{-1} (secondary amide-NH), ν 1750 cm^{-1} (C=O), azomethine (C=N) peak at ν 1608 cm^{-1} , peak at ν 972.12 cm^{-1} (N-N).

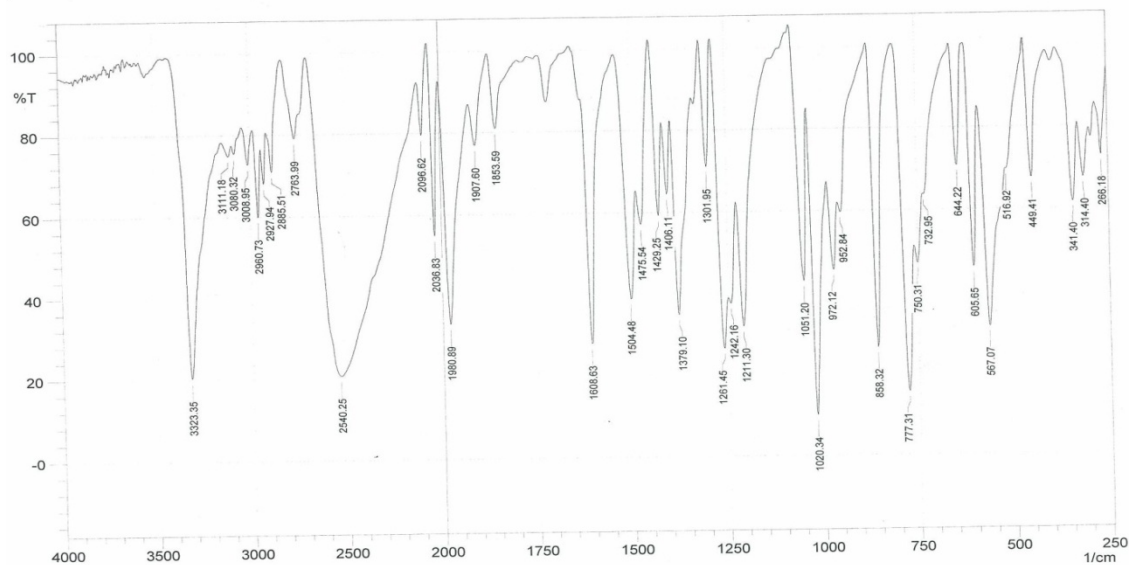
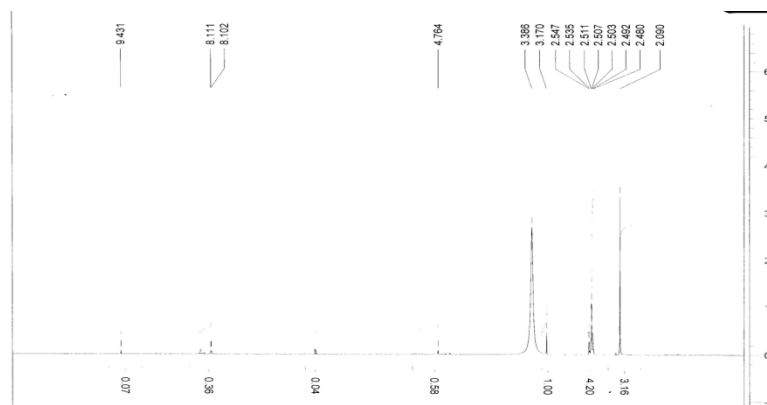


Figure 5: IR Spectrum of Ligand PLCAH

¹H-NMR:

Chemical shift of -OH present on the pyridine ring at 9.431 ppm, -NH proton of 8.11 ppm aromatic (Ar H) at 6.0 ppm, -CH₂OH proton at 4.764 ppm, -CH₂ proton at 2.5 ppm, -CH₃ proton at 2.0 ppm (100).

Figure 6: ¹H NMR of Ligand PLCAH**Characterization of Ni- PLCAH:****LC-MS:**

The liquid chromatographic spectra of Ni-PLCAH complex showed single peak at 0.772 min indicating purity of the complex

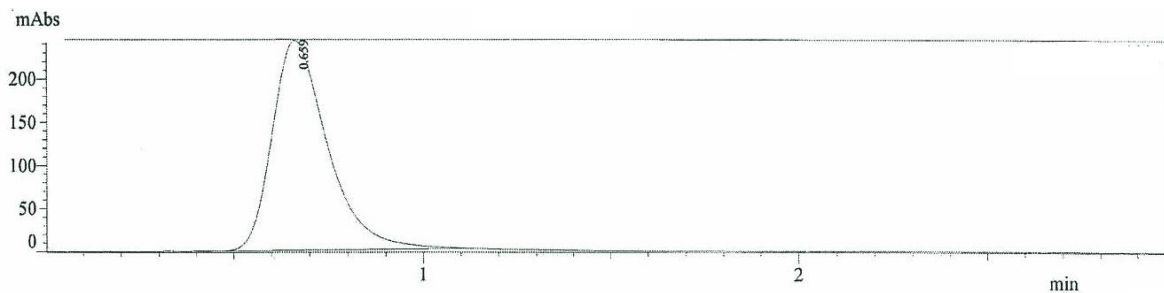


Figure 7: LC-MS of Ni-PLCAH

Mass spectrum of Ni-PLCAH spectrum showed following peaks in its ESI (+) spectrum at m/z 574 (574) which corresponds to $[\text{Ni}(\text{C}_{10}\text{H}_{11}\text{N}_3\text{O}_3\text{Cl})_2]$ which indicates 1: 2 ratio of the complex.

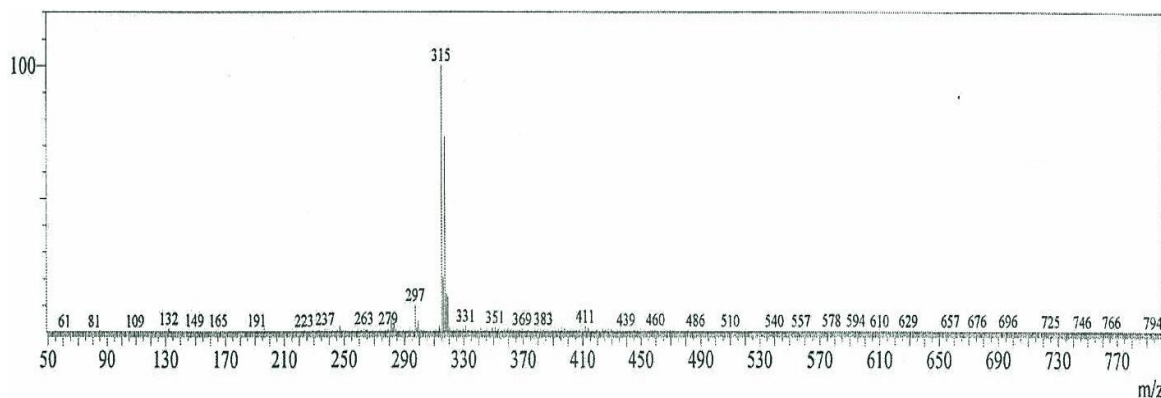


Figure 8: MS of Ni-PLCAH

IR spectra:

Compound	ν Pyridine ring (OH)	2° amide	ν (C=N)	ν (C=O)	ν (N-N)
PLCAH	3323	3111.18	1680.63	1750	972.12
Ni - PLCAH	—	3100.05	1612	1583	975

Table 1: IR Spectra

The IR spectrum of Ni-PLCAH complex showed the following characteristic peaks. The peak at 3323 cm^{-1} disappeared in the complex which corresponds to Pyridine ring (OH) was present in the ligand, this indicates the coordination through oxygen. The peak at 1750 cm^{-1} decreased to 1583 cm^{-1} which corresponds to C=O indicating its coordination through oxygen(98). The decrease in the stretching frequency of azomethine (C=N) from 1680 cm^{-1} to 1612 cm^{-1} shows the coordination through the nitrogen. The peak at 3111 cm^{-1} decreased to 3100 cm^{-1} . The broad peak at 3300 cm^{-1} indicates coordinated water molecule. In the far-IR region peaks corresponding to M-O at 400 cm^{-1} and M-N at 350 cm^{-1} appeared in the complex spectrum.

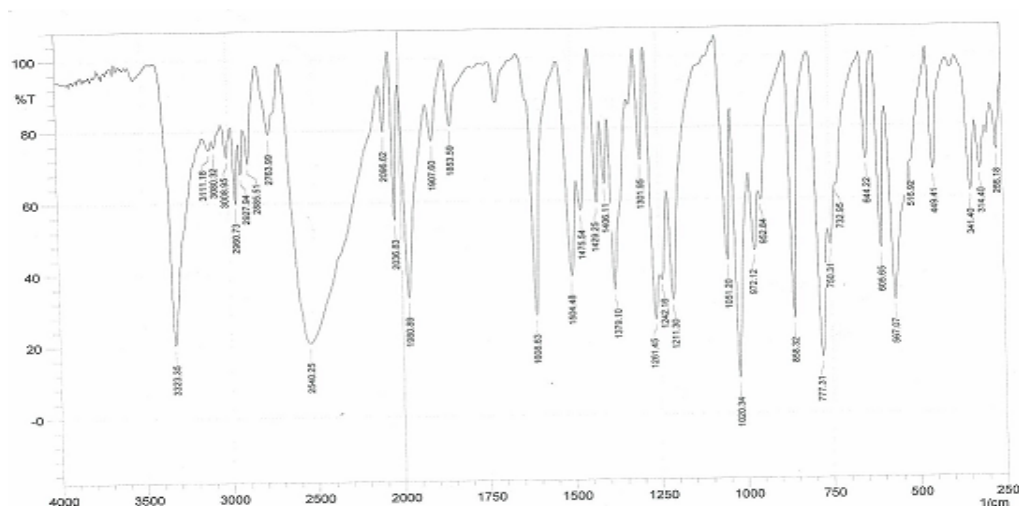


Figure 9: IR Spectrum of Ni-PLCAH

TGA:

The decomposition of the Ni-PLCAH complex has been carried out in two stages there is sudden decomposition of the complex in the first stage from 30°C – 400°C indicating absence of water molecules. Residue is 23 % .

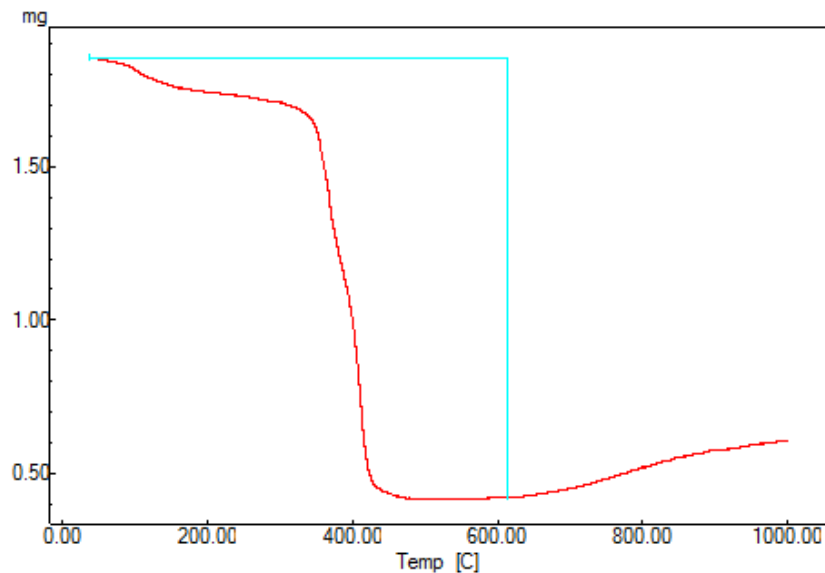


Figure 10: TGA of Ni-PLCAH

U V Spectrum:

The UV spectrum of Ni-PLCAH peak at 385 nm corresponds to d-d transition.

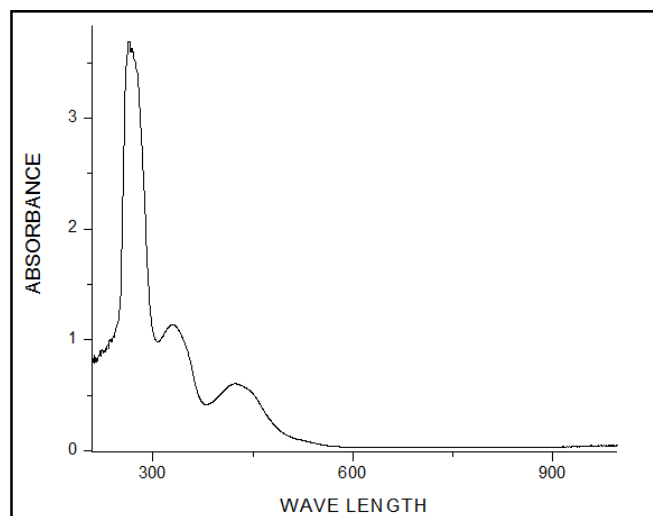


Figure 11: UV Ni-PLACH

DNA Binding studies Ni-PLCAH:

VOL OF DNA	Ea	Ef	Ea-Ef	[DNA]	[DNA]/Ea-Ef
0µl					
20ml	119020158478	271404169177	9187.7415603	$1.836110897 \times 10^{-6}$	$1.998435508 \times 10^{-10}$
40 ml	119020158478	2562.811501	9339.346977	$3.672221795 \times 10^{-6}$	$3.931989896 \times 10^{-10}$
60 ml	119020158478	2520.5030125	9381.6554655	$5.508332692 \times 10^{-6}$	$5.871386678 \times 10^{-10}$
80 ml	119020158478	2505.88335515	9396.2751228	$7.34444359 \times 10^{-6}$	$7.81633519 \times 10^{-10}$
100 ml	119020158478	2424.1126915	9478.0457865	$9.180554487 \times 10^{-6}$	$9.68612591 \times 10^{-10}$

Table 2: DNA Binding studies Ni-PLCAH

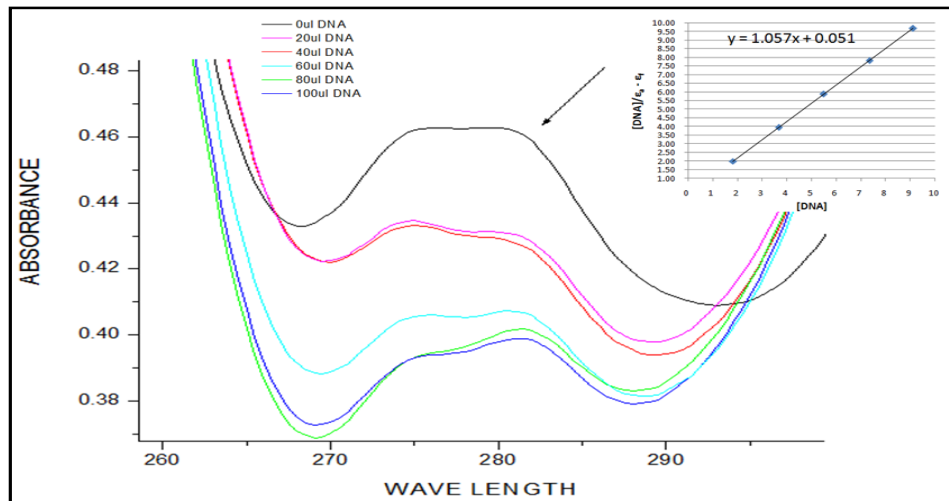


Figure -12: DNA Binding Ni-PLCAH (Kb=2.07×106)

Viscosity of Ni-PLCAH

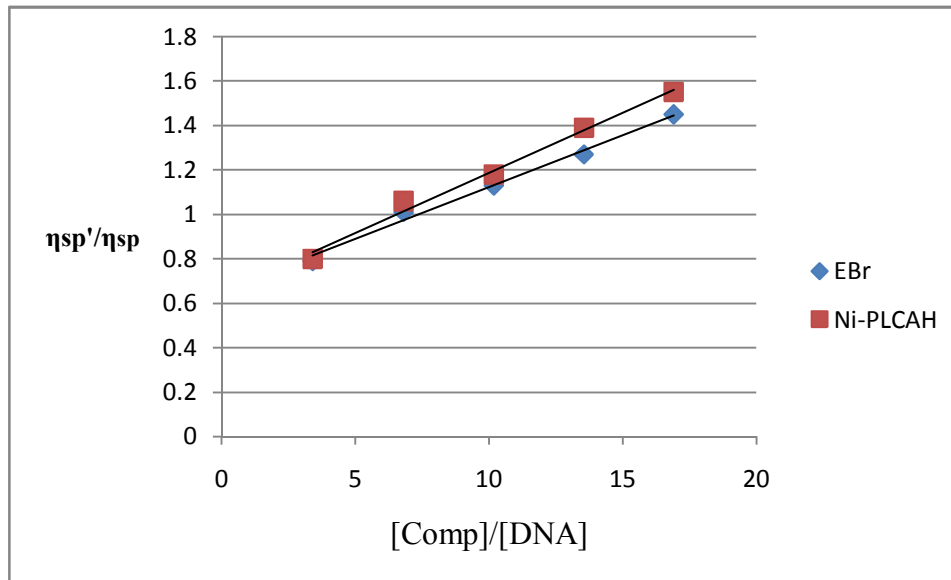


Figure 13: Viscosity studies of Ni-PLCAH

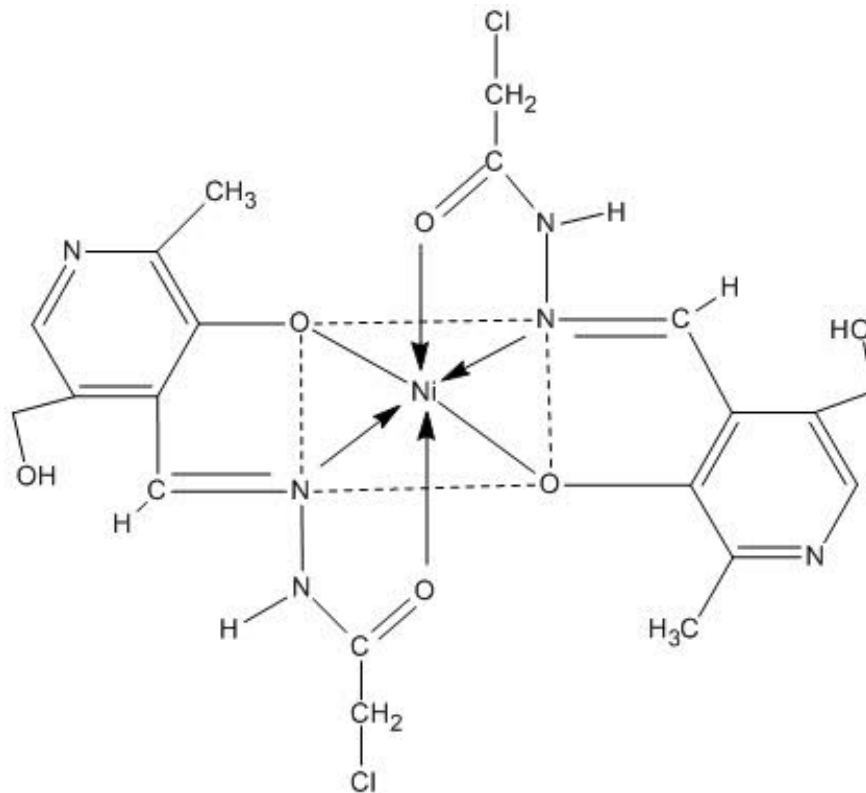


Figure 14: Complex Structure

CONCLUSION

(E-2-chloro-N-(3-hydroxy-5-hydroxymethyl)-2-methylpyridin-4-yl)methylene) acetohydrazide, a derivative of pyridoxal was synthesized by conventional method by treating Pyridoxal hydrochloride with Chloroacetic hydrazide. Ni (II) metal complex was synthesized and characterized using LC-MS, UV, IR and TGA methods. IR spectrum of the complex revealed that the ligand coordinated through 'N' and 'O' donor atoms. The complex was tested for DNA binding activity using Electronic Absorption spectroscopy and Viscosity measurements. The interaction of metal complexes with CT-DNA was studied and the binding constant (K_b) was calculated.

REFERENCES:

1. Lui A, Lumeng L, Aronoff GR, Li TK. Relationship between body store of vitamin B6 and plasma pyridoxal-P clearance: metabolic balance studies in humans. *J Lab Clin Med* 1985; 106:491-497.
2. Gregory JF, 3rd: Bioavailability of vitamin B6 . *Eur J Clin Nutr* 1997; 51(Supl. 1):S43-48.
3. Snell EE. in Fourth international Congress of Biochemistry Vitamin Metabolism 1958; 250-265 (Pergamon, New York).
4. Shane B, Contractor SF. In Human vitamin B6 requirements. Proceedings of a Workshop 1978; 111-128 (National Academy Press, Washington, DC).
5. Wozenski JR, Leklem JE, Miller LT. The metabolism of small doses of vitamin B6 in men. *J Nutr* 1980; 110:275-285.
6. Jansonius JN. Structure, evolution and action of vitamin B6 - dependent enzymes. *Curr Opin Struct Biol* 1998; 8:759-769.
7. Kleijnen J. Knipschild P. Niacin and vitamin B6 in mental functioning: a review of controlled trials in humans. *Biol Psychiatry* 1991; 29:931-941.
8. Selhub J, Bagley LC, Miller J, Rosenberg IH. B vitamins, homocysteine, and neurocognitive function in the elderly. *Am J Clin Nutr* 2000; 71:614S-620S.
9. Mudd SH et al. The natural history of homocystinuria due to cystathionine beta-synthase deficiency. *Am J Hum Genet* 1985; 37:1-31.
10. Selhub J, Miller JW. The pathogenesis of homocysteinemia: interruption of the coordinate regulation by S-adenosylmethionine of the remethylation and transsulfuration of homocysteine. *Am J Clin Nutr* 1992; 55:131-138.



11. Leklem JE. Modern Nutrition in Health and Disease. Lea and Febiger. Pages. Philadelphia. 9. ed. 1998.
12. Lumeng L, Li TK. Vitamin B6 metabolism in chronic alcohol abuse. Pyridoxal phosphate levels in plasma and the effects of acetaldehyde on pyridoxal phosphate synthesis and degradation in human erythrocytes. J Clin Invest 1974; 53:693-704.